SIMULATION EXPERIMENT OF HEAT TRANSFER TUBES FOR ELECTRONIC HEAT ABSORBER IN THERMAL POWER GENERATION SYSTEM OF POWER PLANTS

*Chenhua Wu**
Inner Mongolia Technical College of Mechanics and Electrics, Hohhot, 010070, China.
Email: wuchenhuamchh@126.com

Abstract - The study aims to improve the performance of the thermal power generation system in power plants by analyzing its working principle. The thermal power generation system of large power plants is taken as the research object. The Fluent software is used for simulation experiments. A new optimization method of the rotor structure in the electronic heat absorption equipment and heat exchange pipeline is proposed. By improving the rotor, the heat transfer efficiency of the heat exchange pipeline is greatly improved. Through the relevant research on the thermal power generation system, the rotor's heat transfer performance of the exchange tube is analyzed based on the strong heat transfer convection mechanism. Then the simulation experiment is carried out. Based on the heat transfer mechanism of the combined rotor in the tube path unit, the heat transfer pipe is optimized. The numerical simulation results of rotor heat transfer and fluid flow show that the average resource utilization rate increases with time. The average resource utilization efficiency of the system reaches more than 70% in 45 ms. When the pipe size is 100 mm, the performance of the resistance coefficient is 3.6 before improvement and 2.8 after improvement. When iteration times are 200, the rotor heat transfer of four kinds of pipes reaches the maximum, and the rotor heat transfer of No. 1 pipe with the size of 22 mm can reach 10000W. The research demonstrates the superiority of the proposed heat exchange tube, which provides a theoretical reference for optimizing the heat transfer tube and the efficiency of the thermal power generation system.

Keywords: Thermal power generation system; Electronic heat absorption; Heat transfer tube; Simulation experiment.

1. Introduction

With the development of science and technology, people's living standards have been greatly improved. Various electrical equipment is applied to all walks of people's lives, such as food, clothing, shelter, and transportation [1-3]. Therefore, ensuring the stability of the power system has become the most important task of power companies. The thermal power generation system's performance and endothermic electronic equipment become the focus of power plants.

Among many electronic devices in power plants, electronic heat absorption devices and heat transfer tubes are widely used in chemical, petroleum, and power processing [4]. In heat transfer, the traditional low-pressure heater often gets rusty. The fouling accumulated on the heat transfer tube reduces the heat transfer coefficient of the equipment, resulting in thermal resistance and reducing its heat transfer efficiency.

This increases the cost of power and shortens the service life of the equipment. Therefore, the focus of current research in the industry is to optimize heat transfer equipment design by a simulation experiment. As a result, its performance can be improved, and the goal of energy-saving and emission reduction is achieved.

The key heat transfer technology of heat transfer tubes in a large thermal power system is analyzed, and Fluent software performs the numerical simulation. After the experiment, many factors affecting heat transfer performance are analyzed. A new optimization method of the rotor structure in electronic heat-absorbing equipment and heat exchange pipeline is proposed. After the rotor structure is optimized, the heat transfer efficiency of the heat transfer pipeline is greatly improved. The innovation is that the heat transfer analysis method of the combined rotor in the tube-side unit is used to optimize the heat transfer pipeline. The study provides technical solutions for improving power plants' thermal power generation efficiency.

2. Literature Review

2.1 Thermal Power Generation System of Power Plant

There are many studies on the thermal power generation system of power plants. Ogorure et al. (2018) [5] analyzed the influencing factors of energy supply and the sustainability of multi-generation power plants by investigating agricultural waste power generation. Analyzing the proposed thermal economic environment model of the integrated plant suggests that the power plant should have a net power of 5.226 MW. The energy and exergy efficiencies are 63.62% and 58.46%, respectively. The contribution of the combustion chamber to the overall exergy destruction rate is 15%. This study provides a reference for the sustainable development of the energy environment and the feasibility analysis of the proposed plant. Mahmoudimehr et al. (2019) [6] evaluated the power generation efficiency of solar thermal power plants. Moreover, the developed method is compared with the traditional optimization method. The comparison results show that the power generation value of the multi-objective dynamic programming method is 3.0%–7.5% higher than that of the traditional method. The benefit it brings is also 3.1%–12.6% higher than the traditional method. Rashid et al. (2019) [7] enhanced the process by mixing solar thermal energy with natural gas by referring to the previous study. The results show that solar power generation increases by 70.4%. Real-time optimization can increase solar power generation by 89.7%. Hossain et al. (2020) [8] investigated energy and exergy efficiency in Bangladesh's utility sector based on the data from 2007 to 2016. The results show that the efficiency of power plants varies from 34.9 to 36.3 %, and the exergy efficiency is from 35.0 to 39.2%. Compared with other thermal power plants, the productivity ability of gas-fired power plants is poor, and the exergy sustainability index is constantly changing between 1.54 and 1.64.

The research on the structure and framework of the thermal power generation system is summarized as follows. Eguchi et al. (2021) [9] proposed a decomposition framework for multi-level thermal power generation according to the situation of the western region. The research results show that the power generation efficiency of large power plants is 13% higher than that of small power plants. Tahir et al. (2021) [10] conducted technical research and economic value evaluation on centralized solar thermal power generation. They introduced the solar infrastructure for thermal power generation by taking Pakistan as an example. The results show that under the optimal configuration of solar thermal power plants in Pishin and Quetta, the minimum power cost could be reduced to 14.7 cents/kWh. Saikia et al. (2021) [11] discussed the thermal power generation system of coal and pulverized coal in thermal power plants and applied electron beam technology to the nano-scale study of trace concentration. The research provides a reference for optimizing the thermal power generation system in thermal power plants.

2.2 Design Optimization of Electronic Heat Absorption Equipment and Heat Transfer Tubes

In studying the thermal power generation system, the design of heat exchanger pipes is essential. Ji et al. (2018) [12] designed the shell-and-tube methanol steam reforming reactor through indirect heating steam reforming for hydrogen production. It runs between 250 and 280°C. This proves that the heat transfer area has a greater impact on the performance due to the low operating temperature of the reactor. At the same operating temperature, the methanol conversion rate of the indirect heating reactor is higher than that of an electric furnace reactor. Yongtai et al. (2019) [13] studied the thermal characteristics of the heat storage tube and vacuum tube solar collector. Based on the structure of the heat storage vacuum tube, the internal energy conversion, transmission, and storage theories are formed. The test results show that the average daily conversion efficiencies of parallel and series-parallel prototypes are 56.9% and 48.46%, respectively. Compared with the non-thermal storage prototype, the conversion efficiency of parallel and series-parallel heat storage prototypes increases by 10.9% and 7.8%, respectively. Rui et al. (2020) [14] designed a new thermoelectric conversion device for concentrating solar thermal power generation systems.

The thermoelectric conversion process is realized based on the intelligent lightweight structure. The performance of the device is evaluated by performance and thermodynamic analysis. The proposed device has a higher power-weight ratio. Also, the power generation system with a flexible cable network reflector is light, portable, and small, which is significant for popularizing the distributed layout system. Minghui et al. (2021) [15] discussed the active cooling system of underground electronic equipment in a high-temperature environment. The heat transfer and refrigerant capacity are analyzed. They optimized the design of the micro turbocharger and condenser, evaporator, and capillary tubes. The results show that the temperature of electronic components can be reduced below 163°C under 200°C. The data measured by electronic components at room temperature and 200°C are compared.

The results show that the improved electronic components can normally work at 200°C. Zhu et al. (2021) [16] conducted experiments on the solar phase change-oriented heat storage evaporation and heat pump system and designed a new one. The new system takes the phase change-oriented heat storage tank as the connection center and is coupled with the solar and heat pump systems. The research results show that the heating power consumption of the system is about 72.8% of that of the single heat pump. The daily operating cost is only 41.2% of that of the single heat pump heating system. The average system performance coefficient reaches 3.79. This indicates that the temperature at the heating end is good, which meets the heat energy transfer requirements of electronic equipment.

3. Simulation of Heat Transfer Performance of heat Transfer Tube Combined with a Rotor in the Thermal Power Generation System

3.1 Analysis of the Convective Mechanism of Strong Heat Transfer

In power plants' electronic heat absorption equipment, the flow of fluids can strengthen or weaken the heat conduction. The fluid flow state can be divided into laminar flow [17] and turbulence [18]. After most laminar heat transfer is strengthened, the local flow shows different degrees of turbulence. In the convective heat transfer process, the temperature distribution of laminar flow presents a parabolic shape in the fluid section. The velocity distribution in the fluid channel is chaotic, which strengthens the radial mixing of the fluid in the channel. Under the low Reynolds number, the increase of resistance pressure drop of the turbulent rotor is small. Under the same vicious consumption, the flow field vortex value of the combined rotor of the tube-side unit decreases.

After the heat transfer mechanism is analyzed, it is found that the heat transfer wall has a significant effect on turbulent heat transfer [19]. The fluid has a large streamer in the core area of turbulent flow, and the heat transfer ratio generated by the inertial effect is higher. The heat transfer wall can be divided into three regions, and the thin layer closest to the wall is the viscous bottom.

The laminar flow resistance of fluid in this region is small. The fluid friction resistance is approximately logarithmic distribution in the region away from the wall. In the transition zone between the viscous bottom and the logarithmic region, the frictional resistance of laminar flow and turbulence is roughly equal.

The heat transfer can be carried out by molecular thermal motion. Among the factors affecting the heat transfer temperature of the heat exchanger, the heat load of the heat exchanger has a great influence on the heat transfer coefficient of the instrument. According to the characteristics of the low-pressure heater, the optimized heat exchanger has the following advantages:

First, the optimized heat exchanger can simplify the low-pressure heating model and improve the density distribution of the fluid.

Second, under the same fluid concentration, the improved heat exchanger can analyze the change of fouling acceleration through the speed of the fluid. Based on this, the fouling deposition phenomenon is eliminated in electronic equipment.

Third, at the same speed, the improved power generation system can analyze the concentration of precipitation particles in the fluid. It also analyzes which inlet and outlet of the low-pressure heater are prone to blockage. The heat transfer process is shown in Figure 1:

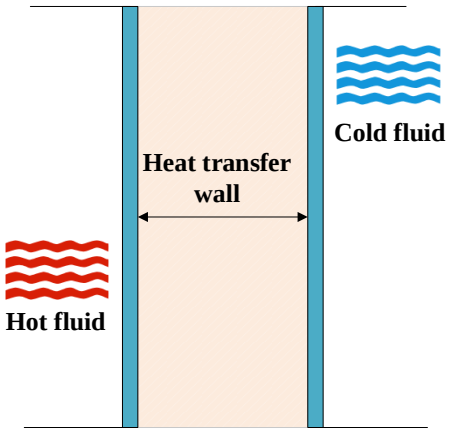

Figure 1: Heat transfer process

3.2 Performance of Heat Transfer Tubes in the Power Generation System

When the heat transfer tube works in the thermal power generation system, the heat is transferred between hot and cold fluids through the convective heat transfer. Inside the heat exchange wall, the heat transfer is enhanced between hot and cold fluids through a convective heat transfer and thermal conduction series [20]. According to heat conservation, when the cold fluid flows in the pipe of the heat exchanger, the hot fluid also flows on the shell of the heat transferer. The heat transfer of the cold fluid in unit time is equal to that of the hot fluid. The heat transfer process is shown in Figure 2.

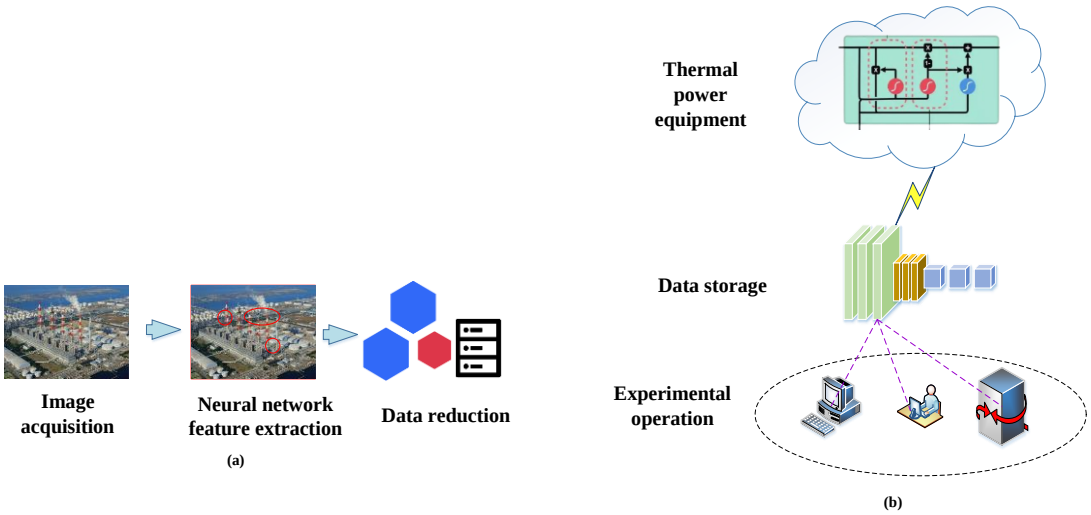

Figure 2: Heat transfer process of casing heat transfer (a. data collection and storage in the heat transfer process; b. the internal circuit of the heat exchanger during heat transfer

For the casing heat transferer, the heat transfer between hot and cold fluids is calculated by Equation (1):

$$Q = m_c C_{p,c}\left(T_{c,\text{out}} - T_{c,in}\right) = m_h C_{p,h}\left(T_{h,in} - T_{h,\text{out}}\right) \quad (1)$$

In Equation (1), m_c and m_h represent the flow rate of hot and cold fluids, and $C_{p,c}$ and $C_{p,h}$ represent the constant pressure specific heat capacity of hot and cold fluids; $T_{c,in}$ and $T_{h,in}$ are the inlet temperature of hot and cold fluids; $T_{c,\text{out}}$ and $T_{h,\text{out}}$ are the outlet temperature of hot and cold fluids. For the heat transfer process between hot and cold fluids, the heat transfer equation is:

$$K = \frac{Q}{\Delta T_m A_o} \quad (2)$$

In Equation (2), ΔT_m is the logarithmic mean temperature difference between hot and cold fluids, and the calculation equation is shown in (3). A_o represents the heat transfer area of the outer surface of the heat exchange tube, and it is calculated by Equation (4). Q represents the overall energy in the heat transfer process.

$$\Delta T_m = \frac{\left(T_{\text{h,in}} - T_{c,\text{out}}\right) - \left(T_{h,\text{out}} - T_{c,in}\right)}{\ln\left[\left(T_{\text{h},in} - T_{c,\text{out}}\right)/\left(T_{h,\text{out}} - T_{c,\text{in}}\right)\right]} \quad (3)$$

$$A_{\text{。}} = \pi d_{\text{。}} l \quad (4)$$

In Equation (4), $d_{\text{。}}$ represents the pipe diameter of the heat transfer tube, and l represents the pipe length. The total heat transfer coefficient in the heat transfer process is calculated by Equations (1) ~ (4), and the convection temperature and flow rate inside and outside the tube are also calculated.

For the casing heat transferer, the convective heat transfer coefficient and the proportional coefficient of the pipe are determined by indirect fitting. According to the experiment, the heat release and heat absorption of the pipe shell are calculated by Equations (5)–(6):

$$Q_o = m_o C_{p,o}\left(T_{o,in} - T_{o,\text{out}}\right) \quad (5)$$

$$Q_i = m_i C_{p,i}\left(T_{i,in} - T_{i,\text{out}}\right) \quad (6)$$

In Equations (5) and (6), m_o and m_i represent the mass and flow rate of the pipeline; $C_{p,o}$ and $C_{p,i}$ represent the constant pressure specific heat capacity of the pipeline ; $T_{o,in}$ and $T_{i,in}$ represent the inlet temperatures of the pipeline and equipment; $T_{o,\text{out}}$ and $T_{i,\text{out}}$ represent the outlet temperatures of the pipeline and equipment; Q_o and Q_i represent the heat release and heat absorption of the pipeline, respectively. During the experiment, the average heat transfer Q_{ave} is:

$$Q_{\text{ave}} = \frac{Q_o + Q_i}{2} \quad (7)$$

The heat release and heat absorption requirement of the pipeline is as follows:

$$\left|\frac{Q_o - Q_i}{Q_o}\right| \le 5\% \quad (8)$$

In the heat transfer process, the expressions of heat transfer and resistance characteristics in the tube are shown in Equations (9)–(10):

$$Nu = c_2 \mathrm{Re}^m \ \mathrm{Pr}^n \left(\frac{p}{\pi d_{\text{i}}}\right)^{\text{a}} \left(\frac{D_{\text{r}}}{d_{\text{i}}}\right)^{\text{b}} \quad (9)$$

$$f = c_1 \mathrm{Re}^{\text{r}} \left(\frac{p}{\pi d_{\text{i}}}\right)^{\text{c}} \left(\frac{D_{\text{r}}}{d_{\text{i}}}\right)^{\text{d}} \quad (10)$$

In Equations (9) and (10), $c_1, c_2, a, b, c, d, r, m, n$ are different experimental parameters, and they are obtained by the experimental data and used for statistical regression. Nu and f represent the heat transfer and resistance characteristics of the pipeline, Re and Pr represent the Nusselt number

and Reynolds number of the medium in the pipeline, $\left(\frac{D_r}{d_i}\right)$ represents the convective heat transfer coefficient of the pipeline, $\left(\frac{p}{\pi d_i}\right)$ represents the effective heat transfer coefficient of the fluid in the pipeline.

The simulation of the cold and hot alternation of the heat exchange tube in the system is shown in Figure 3.

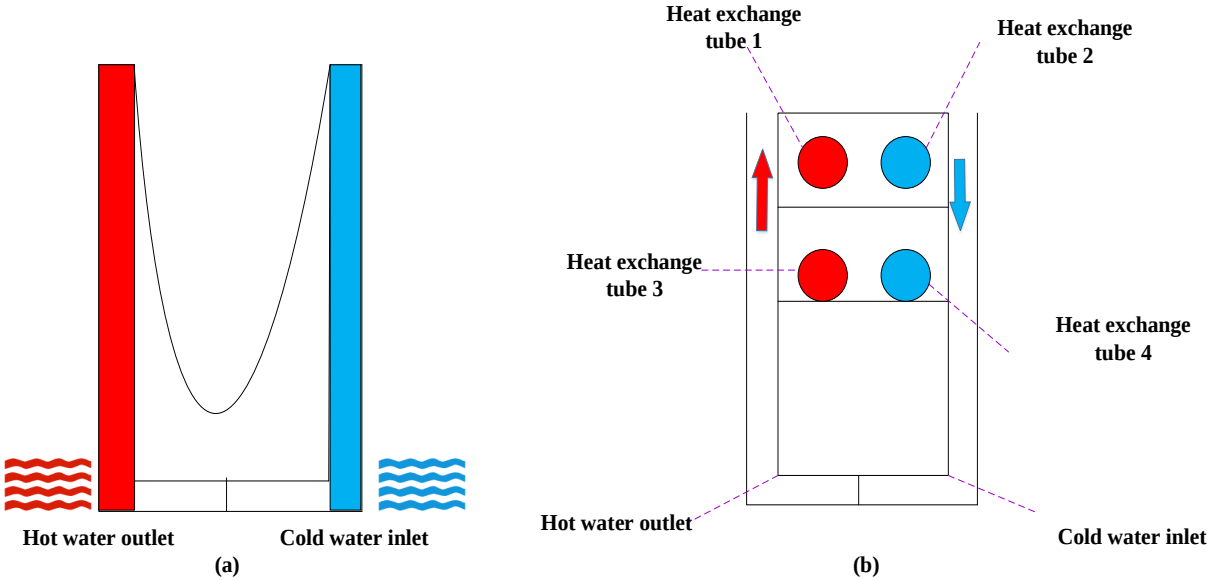

Figure 3: Simulation of heat-cooling alternation of the heat exchange pipeline in the system (a. the heat transfer model of the heat exchange pipeline before the heat exchange rotor is added; b. heat transfer model of heat exchange pipe after the rotor is added)

3.3 Experimental Process Analysis and Data Processing

In the data simulation experiment of the thermal power generation system, the hot water is first delivered into the heat transfer pipe from the hot water tank. After countercurrent heat transfer, the cooled water flows into the heating box for reheating, and the heat is supplemented by heating. Moreover, the refrigerant is used in the heat transfer pipe. Through the cold water of the pump, the refrigerator is cooled. The flow meter and the measurement control system are used to collect the sensing data. In the experiment, the following experimental steps are required:

First, before the experiment, the pressure difference meter of the circulating water pump is operated to make the value of the dial zero.

Second, the heat transfer pipes to be tested are split, and the combined rotor is taken out for testing.

Third, the hot water switch is first opened to heat the cold water in the water tank, and the flow rate of hot water is adjusted to keep the flow rate constant during the experiment.

Fourth, when the hot water reaches a constant temperature, turn on the refrigerator to keep the cold-water flow stable and start measuring data.

Fifth, the cold-water flow is adjusted to record the heat transfer value of the heat transfer tube when the cold water increases or decreases. The corresponding data are recorded.

Sixth, after the data recording is completed, the heating and cooling operations of the device are stopped. After the rotor is replaced, the above operation steps are repeated, and the experimental data are recorded. Data collection is shown in Figure 4:

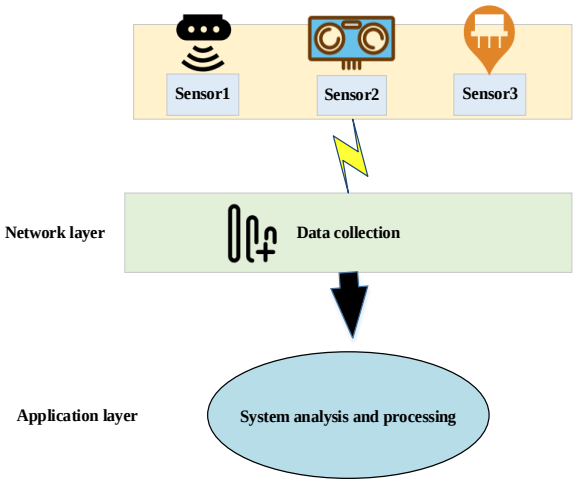

Figure 4: Data collection

3.4 Simulation Experiment

The simulation experiment of the heat transfer efficiency of the low-pressure heater is conducted to verify the performance of the thermal power system of the electronic plant. The stainless-steel heat transfer tube is used in the experiment according to the resistance characteristics of the combined rotor. The size of the stainless-steel tube is 25 mm × 3.5 mm. The data obtained in the experiment are the actual power generation data of a thermal power plant.

The experimental data are obtained by installing temperature sensors at the inlet and outlet of the tube. The heat transfer tube needs to learn to put different generators into identifiable modes. Gradient vanishing is solved by modifying the loss function.

A multi-generator combination method is designed to avoid mode collapse. Two or more generators and a discriminator are used.

Each generator shares the same input data, and synchronous training can improve the convergence speed of the model. Some intrusion detection evaluation data are selected as data sets to verify the audit data of the power generation system and the performance of the heat transfer tube.

In addition, computer software is used for data performance analysis. In terms of software, the operating system is Linux 64 bit, the Python version is Python 3.6.1, and the development platform is PyCharm. On hardware, the central processor is Intel Courier i7-7700 @ 4. 2 GHz 8 – core, and the memory is Kingston ddr4 2400MHz 16G. The simulation software is Fluent. Four different pipes of 22mm, 100mm, 150mm, and 200mm are selected to compare the performance of the tube-side composite rotor. The numerical analysis method is used to compare the performance of the heat transfer tube.

The equipment and scene of the simulation experiment are as follows:

(a) (b)

Figure 5: Simulation experiment scene (a. thermal power generation equipment of power plants; b. heat transfer pipeline of the power generation system)

4. Results

4.1 Numerical Simulation Results

Through simulation experiments, the average reaction time and average resource utilization rate of thermal power generation systems in a power plant are evaluated.

And the relationship between the data stored in the system and the iteration times of the model is tested, and the results are shown in Fig.6.

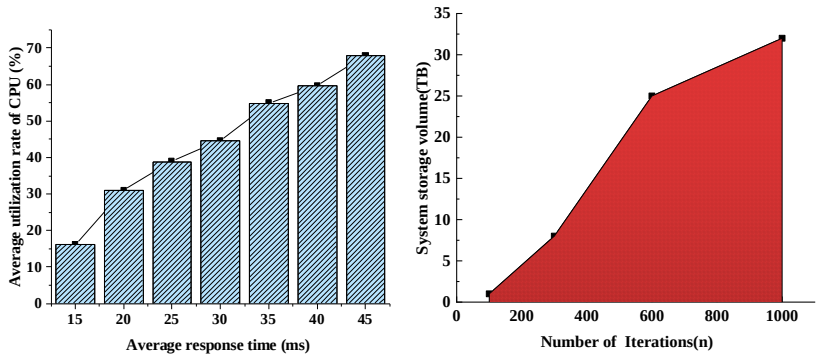

(a) (b)

Figure 6: Simulation test results of the relationship between the data storage of power generation system and the number of model iterations (a. System average reaction time and resource utilization rate; b. Relationship between the amount of data stored in the system and the iteration times of the model)

Figure 6 (a) shows that the longer the reaction time of system consumption is, the higher the average resource utilization rate is. At 15ms, the average resource utilization efficiency of the central processing unit (CPU) is only 15%. The average resource utilization rate increases gradually with the increase in system reaction time. The average resource utilization efficiency of the system reaches more than 70% at 45ms, which greatly improves the power generation efficiency of the thermal power generation system. When the power generation loss time of the system is reduced, the heat loss of the heat transfer tube and the energy loss of the power plant are reduced.

Figure 6 (b) shows that with the increase in the iteration times of the model, the data stored in the system grow. The size only reaches 10TB when the iteration times of the model are 400. With the increase in iteration times, the system begins to be optimized.

After 1000 iterations, the size of the stored data can reach more than 30 TB. A larger data size means that the power generation system can handle more power generation tasks in a shorter time, and the system efficiency is greatly improved.

4.2 Numerical Simulation Results

Four heat transfer pipelines with different sizes of 22 mm, 100 mm, 150 mm, and 200 mm are selected for the simulation experiment. Moreover, the performance of different heat transfer pipelines before and after improvement is compared. Among them, pipeline 1 is 22 mm, pipeline 2 is 100 mm, pipeline 3 is 150 mm, and pipeline 4 is 200 mm. The changes in pipeline resistance coefficients before and after the improvement of the system are shown in Figure 7. The trend of the rotor heat transfer of different heat transfer pipelines with different iteration times is shown in Figure 8.

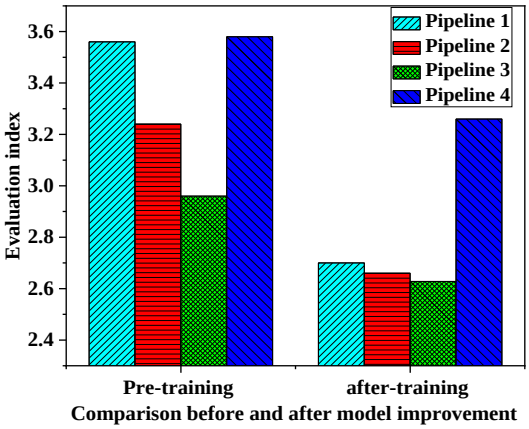

Figure 7: Comparison of resistance coefficients of different heat transfer tubes before and after improvement

Figure 7 shows that the resistance coefficient of different pipelines is improved after system improvement. The resistance coefficients of pipeline 1 are 3.6 and 3.4 before and after system improvement. The effect of pipeline 2 is the most obvious, and its resistance coefficients are 3.6 and 2.8 before and after improvement.

The resistance coefficients of pipeline 3 and pipeline 4 are 3.3 and 3.0, respectively. After system optimization, they are reduced to about 2.7. This shows that the improved thermal power generation system has built-in rotors, which helps to improve the performance of heat transfer tubes and reduce the energy loss in power generation.

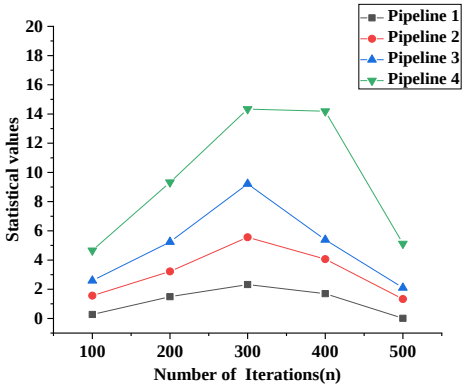

Figure 8: Curves of rotor heat transfer in different heat exchange tubes with the iteration times of the model

Figure 8 shows that under the same iteration times, the heat transfer capacity of the rotor placed in heat exchange pipe 1 is higher than that of other pipes. When the iteration times are 100, there is little difference in the rotor heat transfer. With the increase of the iteration times, the rotor heat transfer of the four pipelines reaches the maximum when the iteration times are 300. The rotor heat transfer capacity of pipeline 1 can reach 10,000W. Its heat transfer capacity is the largest, while the rotor heat transfer capacity of pipeline 4 is only 2,000W. Its rotor heat transfer capacity is the smallest. When the iteration times of the model are greater than 300, the heat transfer capacity of the rotor begins to decrease. Thus, the heat transfer of the rotor heat transfer tube in the power generation system is inversely proportional to the resistance coefficient of the light tube.

The increase of the light tube's resistance coefficient makes the rotor's heat transfer begin to decrease. Therefore, when iteration times of the model are 300, the power generation capacity of the power generation system is the largest, and the system performance is the best.

Further, it studies the heat absorption and heat dissipation performance of the heat absorber pipe. In order to do so, the measured and simulated temperatures are compared by considering the thermocouple numbers. Data are collected from 50 measurement points and sorted out. Here, ten data points are taken as a group of data, and the results are shown in Figure 9 (a). Additionally, the power generation and heat absorption changes at different electronic heat absorber pipe sections are simulated. The temperature changes at each pipe position with time are obtained, as shown in Figure 9 (b).

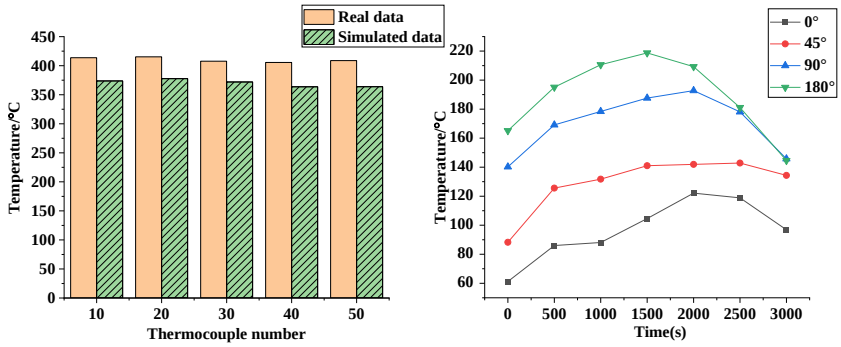

(a) (b)

Figure 9: Temperature change curves of different heat absorber numbers and cross-sections (a. data comparison of measured temperature and simulated temperature of different thermocouple numbers of heat absorber; b. data curve of temperature change with time at different cross-sections of heat absorber pipeline)

From the data comparison image of measured temperature and simulated temperature of different thermocouple numbers of heat absorber in Figure 9 (a), among the 50 measurement points, the error between the measured and simulated value of three groups of experimental data points is within 5%. The error is no more than 10% on the other two groups of data points. Therefore, the heat loss on the back of the heat absorber is not much, and the simulation performance of the system can achieve the perfect expected effect.

In Figure 9 (b), different curves represent different section positions in the pipeline. The black curve represents the pipeline has 0 degrees angle with the horizontal position of the section. The red curve means the pipeline has an angle of 45 degrees with the horizontal position of the section. By comparison, the blue curve indicates that the pipe has an angle of 90 degrees from the horizontal position of the section. Lastly, the green curve implies that the pipe has an angle of 180 degrees with the horizontal position of the section. Overall, with the extension of time, the temperature at all positions in the generator heat absorption pipeline will show an upward trend. The changing trend of temperature distribution at the horizontal position of the heat absorber pipeline is even.

The greater the angle difference with the horizontal position of the heat absorber pipe is, the more obvious is the temperature rise and change trend. Among them, the temperature change of the pipe position with an included angle of 180 degrees with the horizontal position of the section shows a trend of first-rise-then-decline.

5. Conclusions

With the development of the social economy, electricity has become an indispensable energy resource. The thermal power generation system of large power plants is taken as the research object to optimize power plants' thermal power generation system. A new optimization method of the rotor structure in electronic heat absorption equipment and heat transfer pipe is proposed through experimental, numerical simulation, and case application methods. By improving the rotor, the heat transfer efficiency of the heat transfer pipe is

greatly improved. Based on the analysis of the heat transfer mechanism of the combined rotor in the tube path unit, the heat transfer pipe is optimized. The numerical simulation results of rotor heat transfer and fluid flow show that the average resource utilization rate increases gradually with the increase of the reaction time.

The research has practical application value for improving the efficiency of thermal power generation systems in power plants. However, some shortcomings are unavoidable:

(1) The model of a low-pressure heater can be further improved by setting operating parameters and grid network for fouling simulation. In rational modeling, the division of the fluid region in the pipe should be strengthened, and the data transfer relationship should be simulated within different fluid regions.

(2) In the heat transfer tube of the electronic heat absorption equipment, the deposited fouling causes great damage to the performance of the heat transfer tube. A better model should be implemented to determine the position of the fouling deposition, which is also the direction that should be improved in the later research.

References

[1] Howard B. E. (2020) High-risk aerosol-generating procedures in COVID-19: respiratory protective equipment considerations. Otolaryngology–Head and Neck Surgery, 163(1), 98-103.

[2] Vasilyevich P. S., Aleksandrovich S. D. (2021) Methods to improve the efficiency of the business process of repairing power-generating equipment. International Review, (1-2), 161-171.

[3] Gubin P. Y., Oboskalov V. P. (2021) The initialization of initial generating equipment maintenance schedules while a heuristic method is used. Vestnik of Samara State Technical University. Technical Sciences Series, 29(2), 6-23.

[4] Hinrichsen T. F., Chan C. C. S., Ma C., et al. (2020) Long-lived and disorder-free charge transfer states enable endothermic charge separation in efficient non-fullerene organic solar cells. Nature communications, 11(1), 1-10.

[5] Ogorure O. J., Oko C. O. C., Diemuodeke E. O., et al. (2018) Energy, exergy, environmental and economic analysis of an agricultural waste-to-energy integrated multi-generation thermal power plant. Energy conversion and management, 171, 222-240.

[6] Mahmoudimehr J., Sebghati P. (2019) A novel multi-objective Dynamic Programming optimization method: Performance management of a solar thermal power plant as a case study[J]. Energy, 168, 796-814.

[7] Rashid K., Safdarnejad S. M., Powell K. M. (2019) Process intensification of solar thermal power using hybridization, flexible heat integration, and real-time optimization. Chemical Engineering and Processing-Process Intensification, 139, 155-171.

[8] Hossain S., Chowdhury H., Chowdhury T., et al. (2020) Energy, exergy and sustainability analyses of Bangladesh's power generation sector. Energy Reports, 6, 868-878.

[9] Eguchi S., Takayabu H., Lin C. (2021) Sources of inefficient power generation by coal-fired thermal power plants in China: A metafrontier DEA decomposition approach. Renewable and Sustainable Energy Reviews, 138, 110562.

[10] Tahir S., Ahmad M., Abd-ur-Rehman H. M., et al. (2021) Techno-economic assessment of concentrated solar thermal power generation and potential barriers in its deployment in Pakistan[J]. Journal of Cleaner Production, 293, 126125.

[11] Saikia B. K., Hower J. C., Islam N., et al. (2021) Geochemistry and petrology of coal and coal fly ash from a thermal power plant in India. Fuel, 291, 120122.

[12] Ji H, Lee J, Choi E, et al. (2018) Hydrogen production from steam reforming using an indirect heating method. International journal of hydrogen energy, 43(7), 3655-3663.

[13] Yongtai H., Lixian X., Yaohua Y. (2019) Study on design and thermal characteristics of vacuum tube solar collector intubated with heat storage tube. International Journal of Energy Research, 43(13), 7409-7420.

[14] Rui X., Zheng F., Zheng T., et al. (2020) Conceptual design of a new thermal-electric conversion device in lightweight concentrating solar thermal power system. Energy Science & Engineering, 8(1), 181-202.

[15] Minghui W., Wei C., Mingze X., et al. (2021) Active cooling system for downhole electronics in high temperature environments. Journal of Thermal Science and Engineering Applications, 1-16.

[16] Zhu C., Li B., Yan S., et al. (2021) Experimental research on solar phase change heat storage evaporative heat pump system. Energy Conversion and Management, 229, 113683.

[17] Luo X., Zhang W., Dong H., et al. (2021) Numerical analysis of heat transfer enhancement of fluid past an oscillating circular cylinder in laminar flow regime. Progress in Nuclear Energy, 139, 103853.

[18] Nguyen K. A., Azevedo F. S., Papendieck A. (2021) No longer an imaginary case: Community, plans, and actions in canoeing rapids. Journal of the Learning Sciences, 30(4-5), 529-575.

[19] Zhang P., Rao Y., Xie Y., et al. (2021) Turbulent flow structure and heat transfer mechanisms over surface vortex structures of micro V-shaped ribs and dimples. International Journal of Heat and Mass Transfer, 178, 121611.

[20] Briongos J. V., Gómez-Hernández J., González-Gómez P. A., et al. (2018) Two-phase heat transfer model of a beam-down gas-solid fluidized bed solar particle receiver. Solar Energy, 171, 740-750